01 Jan 1991

Fe^{q+}+ H, $H_2$and He Electron Loss And He^{2+}+ H(N = 1, 2) Electron Capture Cross Sections: Processes Of Interest In Fusion Plasmas

D. R. Schultz

L. Meng

C. O. Reinhold

Ronald E. Olson
Missouri University of Science and Technology, olson@mst.edu

Recommended Citation

D. R. Schultz et al., "Fe^{q+}+ H, $H_2$and He Electron Loss And He^{2+}+ H(N = 1, 2) Electron Capture Cross Sections: Processes Of Interest In Fusion Plasmas," *Physica Scripta*, vol. 1991, no. T37, pp. 89 - 93, IOP Publishing; Royal Swedish Academy of Sciences, Jan 1991.
The definitive version is available at https://doi.org/10.1088/0031-8949/1991/T37/015

Physica Scripta

Fe^{q+} + H, H_2 and He Electron Loss and He^{2+} + H(n = 1,2) Electron Capture Cross Sections: Processes of Interest in Fusion Plasmas

To cite this article: D R Schultz *et al* 1991 *Phys. Scr.* **1991** 89

Physica Scripta. Vol. T37, 89–93, 1991.

Fe^{q+} + H, H_2 and He Electron Loss and He^{2+} + H(n = 1,2) Electron Capture Cross Sections: Processes of Interest in Fusion Plasmas

D. R. Schultz, L. Meng, C. O. Reinhold and R. E. Olson

Department of Physics and Laboratory for Atomic and Molecular Research, University of Missouri-Rolla, Rolla, Missouri 65401 U.S.A.

Received October 9, 1990; accepted January 14, 1991

Abstract

Cross sections have been calculated utilizing the classical trajectory Monte Carlo method for collisional processes of special interest to plasma fusion research. Specifically, H, H_2 and He total electron loss cross sections for the impact by Fe^{q+} $(1 < q < 26)$ impurity ions, in the energy range of 50 to 500 keV/u, are presented. These results illustrate a clear departure for low charge states ($q \lesssim 10$) from scaling of the cross section with projectile charge (q). Further, cross sections for electron capture from both the ground and $n = 2$ states of H by 30 to 100 keV/u He^{2+} impact are tabulated as function of final n-level, yielding information for neutral beam heating models.

1. Introduction

To be certain, the ultimate goal of plasma fusion experiments is the production of energy in amounts greater than that required to produce fusion in the first place. However, even though the critical step in which energy is released is a nuclear reaction, fusion experiments present a tremendous challenge to atomic physics in that many of the difficulties in obtaining this goal are related to the various energy loss mechanisms associated with atomic collisions in the plasma. Here we address two specific needs of the current world plasma fusion program, which includes the design of the Interntional Thermonuclear Experimental Reactor (ITER), by presenting calculations of total electron loss cross sections for collisions for Fe^{q+} ions with H, H_2 and He, and electron capture cross sections for He^{2+} colliding with H.

Specifically, detailed knowledge of these atomic processes is crucial since it provides the means of diagnosing the conditions which are present in the fusion plasma and also play an important role in getting such heating schemes as neutral beam injection to work in an optimal fashion. Quantitatively determined cross sections allow plasma models to be created to help predict the performance of existing devices and to aid in the design of new experiments. Since atomic collision experiments to deduce all of the possible reactions is prohibitively time consuming and expensive, theoretical estimates, when properly benchmarked with sufficient agreement with experiment, must provide most of the data required. Furthermore, both theoretical and experimental work to determine the required data often leads to valuable insight, such as the discovery of scaling laws, which reduces the number of cross sections which actually need be measured or calculated.

In particular, some of the most deleterious energy loss mechanisms in the fusion plasma are due to the presence of impurity ions, such as iron which is sputtered from the containment vessel by neutrals which escape magnetic confinement. These ions enter the plasma, robbing it of energy, and therefore lowering its temperature, by suffering inelastic collisions with plasma ions. These collisions produce various stages of ionization and excitation of the impurity ion and cause bremsstrahlung and line radiation losses. Also, of great importance for neutral beam heating studies is knowledge of the results of charge transfer collisions between the injected neutral hydrogen beam and the plasma components, notably He^{2+}. Line radiation from excited states formed by these electron capture processes result in impairment of the neutral beam heating efficiency. A useful side-effect of these processes is diagnosis of the depth of penetration of the beam through optical detection of the pattern of radiation.

The results presented here have been obtained using the classical trajectory Monte Carlo (CTMC) technique, a method which has been successfully applied to a number of plasma fusion processes heretofore. However, two significant advances of this technique have been necessitated by studies of the present type, namely the development of means to represent accurately the effects of projectiles carrying many electrons, and the creation of a model for molecular hydrogen. The CTMC method and these new extensions are briefly described in Section 2 and the results are presented and discussed in Section 3.

2. Theoretical method

The classical trajectory Monte Carlo technique is, in brief, a method in which a large ensemble of projectile-target configurations is sampled to simulate the ion-atom collision, and consists of three steps. In the first, the position and momentum of the electron of the target is chosen in a Monte Carlo fashion from an initial classical distribution whose properties closely resemble the correct quantum mechanical electronic distribution. Next, the trajectories of the projectile, target electron and target core throughout the collision are determined by iteratively solving the classical equations of motion. Finally, subsequent to the integration into the asymptotic regime, the relative energies of each of the particles are found to determine what, if any, reaction occurred. Cross sections may then be computed, along with a measure of the statistical uncertainty of the result, in a particle counting method.

The basic CTMC technique applied to atomic collisions has been originally described by Abrines and Percival [1] and subsequently by Olson and Salop [2], Olson [3] and others. The application of this method to state selective electron capture has been given by Becker and MacKellar [4] and has been extensively exercised for multiply charged ion impact of the ground state of hydrogen. In particular, Olson [5] has described the dominant features of the product n,l distribution after capture for multiply charged ion impact at 50 and 100 keV/u and Olson and Schultz [6] provided a detailed extension of that work for C^{6+} and O^{8+} impact over the energy range of 40 to 140 keV/u.

In order to apply this technique to the impact by partially stripped projectiles a method in which the static screening of the projectile by the electrons which it carries has been incorporated. In this case, the projectile – target-electron interaction is treated by using a Hartree–Fock model potential. Alternatively, this interaction could be represented by a simple, screened Coulomb parameter, however, the model potential has the advantage of possesing the correct asymptotic behaviors at both large and small separations of the projectile and target electron. Thus, it is presumed that this method would more realistically describe the effect of the partially stripped projectile in, especially, close collisions with the target, and when the projectile carries many electrons. This model potential method has been described in detailed by Reinhold *et al.* [7] for the case of ionization of helium by C^+ ions. In that work excellent agreement was found with experimental measurements of the doubly differential electron emission cross sections, providing a stringent test.

Another significant advance which we take advantage of in this work is the utilization of the first CTMC model implemented for ion-molecule collisions. This model, developed by Meng *et al.* [8] has been demonstrated to provide an excellent description of electron capture and ionization in fully stripped ion-H_2 collisions at intermediate energies. In the present work, this treatment too has been extended to include model potential interactions between the projectile and target electrons to treat impact by partially stripped ions.

Application of these CTMC models is appropriate because of their demonstrated validity in the intermediate collision energy regime. In this regime, the projectile velocity is comparable to the orbital velocity of the target electron. Furthermore, this energy range presents difficulties for methods based on quantum mechanical basis set expansion since such large numbers of states are required. Fortunately, the leading quantum effects in this regime enter in the initial state of the collision system, as approximated in the CTMC method, and the subsequent dynamic evolution may be well represented by classical mechanics.

3. Results and discussion

3.1 Fe^{q+} + H, H_2 and He: total target electron loss

One of the primary species of impurities present in fusion plasmas are ions of iron. Iron, the major constituent of steel, is sputtered from the vessel wall when neutrals escape magnetic confinement. Upon entering the plasma, the iron ions undergo many inelastic collisions, lowering the plasma temperature, and creating in the process a broad distribution of charge states. Thus, important information for modelers is the ionization and charge transfer cross sections for iron ions colliding with the primary plasma components at energies corresponding to the plasma ion temperatures and under neutral beam injection. Accurate treatment of electron capture by the iron ions is a difficult n-body problem since partially stripped iron contains as many as twenty five electrons. Such a calculation must properly account for the capture of additional electrons and the proper relaxation of the final electronic distribution. We therefore direct our attention in this work to the more tractable task of treating the electron loss process from the few electron cases, H, H_2 and He, and consequently consider an energy regime high enough so that the capture probability for the low charge states of iron are negligible.

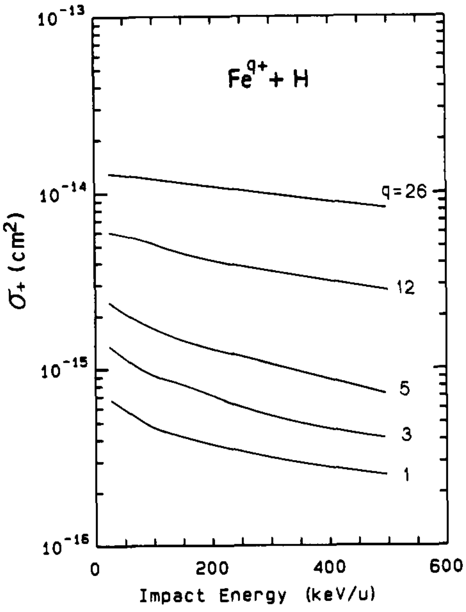

Fig. 1. The total cross section for electron loss (sum of ionization and charge transfer) in collisions of Fe^{q+} and atomic hydrogen for several projectile charge states as a function of impact energy.

To this end we consider 50 to 500 keV/u collisions of Fe^{q+} with these targets and report the total cross sections for target electron loss. For example, in Fig. 1 we display the electron loss cross section, which is the sum of ionization and electron capture for Fe^{q+} colliding with H, for several different charge states q. We emphasize that for the lower charge states, the capture probability is very small for these impact energies and the complications of treating the capture of an electron by an ion with many electrons are avoided. For the higher charge states, the capture probability is not so small but, since the projectile electrons occupy only the inner shells in this case and capture proceeds to the vacant outer shells at these energies, such difficulties do not arise.

As this figure indicates, the electron loss cross section drops off rather slowly in this energy range and that the

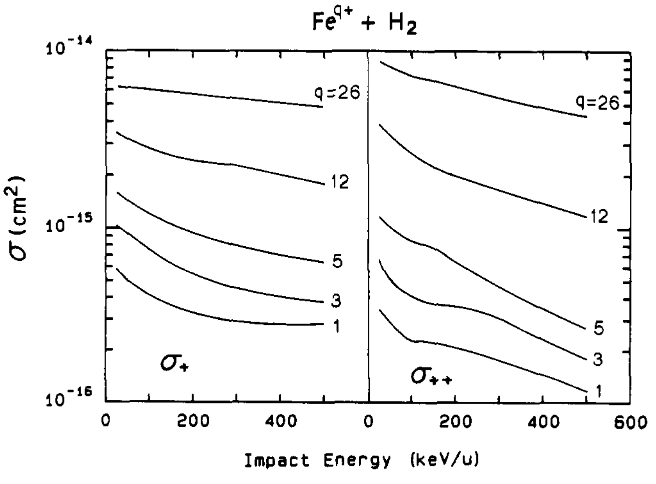

Fig. 2. The total cross section for electron loss (production of H_2^+ and H_2^{++}) in collisions of Fe^{q+} and molecular hydrogen for several projectile charge states as a function of impact energy.

magnitude of the cross section increases with charge state. One may readily verify that the cross section for charge state q is on the order of q times the cross section for Fe^+. Similar behavior is evidenced for molecular hydrogen, as illustrated by Fig. 2. Here, we display both the single and double electron loss cross sections, which represent the sum of ionization and electron capture, and the sum of double ionization, transfer ionization and double electron capture, respectively. We note that, contrary to what one might assume, the single electron loss cross sections for the impact of H_2 are not simply twice that for impact of H. Indeed, for the lower iron ion charge states, the single electron cross sections for H and H_2 are nearly equal, and are smaller by about 50 percent for the higher charge states [8]. Also, we note that the cross section for double electron loss is comparable in magnitude to the single electron loss cross section. In Fig. 3 the same quantities are displayed for a helium target. Reflecting the increased binding energy over that present in H_2, the helium electron loss cross sections are about half their analogs in H_2.

As alluded to in Section 1, a very useful tool which to some extent eliminated the need to compute or measure the electron loss cross section for each ion and ionic charge state has been the discovery of a simple scaling law. In fact, Olson *et al.* [9] found that in collisions of heavy, highly stripped ions with H, the electron loss cross sections reduced to a single curve if the cross section divided by the charge state is plotted versus the impact energy per nucleon divided by the charge state. The validity of the scaling for highly charged ions impinging on the rare gases was subsequently confirmed by Schlachter *et al.* [10, 11]. Further, similar scalings in terms of reduce quantities have been demonstrated for electron capture and ionization (see Graham *et al.* [12], Janev and Hvelplund [13] and Phaneuf *et al.* [14]).

To explore whether or not a simple scaling exists in this case, in Fig. 4 is displayed the reduced electron loss section for Fe^{q+} + H plotted as a function of the reduced energy. Clearly, the cross sections for all charge states do not fall on a single curve, however, for the highest charge states, the cross sections do tend to group more closely. That is, the largest departures from this scaling occur for the lower charge states. This departure is illustrated in more detail in Figs. 5 through 7 where the total electron loss cross sections are plotted for each of the three target gases as a function of the iron charge state. In these figures is also displayed curves representing the electron cross sections for fully stripped ions of charge equal to the ionic charge of the iron ion.

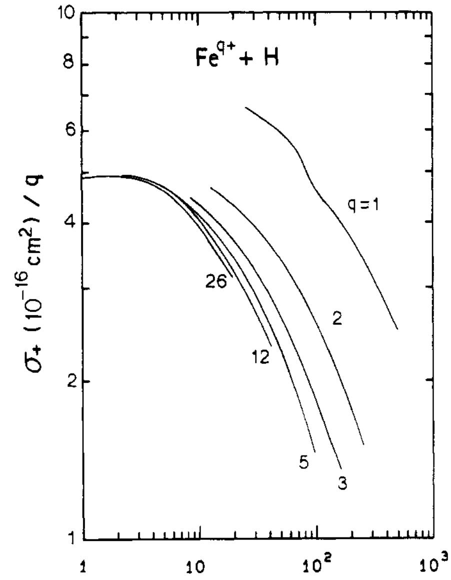

Fig. 4. The scaled cross section for electron loss (σ_+/q) in collisions of Fe^{q+} and atomic hydrogen for several projectile charge states as a function of the scaled energy (E/q).

For example, in Fig. 5 for atomic hydrogen, one notes that for charge states below $q = 5$ the Fe^{q+} ions have a larger reduced cross section than do their fully stripped counterparts. For higher charge states, the fully and partially stripped ions produce essentially the same reduced electron loss cross section. Similarly for H_2 and He (Figs. 6 and 7), iron ion charge states less than six or seven evidence an enhancement over the fully stripped ions, the largest difference occurring for $q = 1$. For the low charge states of the iron ion, this enhancement over the cross section for impact by fully striped ions of equal charge occurs due to the fact that in the collisions, the projectile core may be penetrated, exposing a much greater charge. For example, in a very close collision of low charge state iron ion with an atom, it is not the asymptotic charge q that is experienced by the electron but rather more nearly the nuclear charge. This effect of core

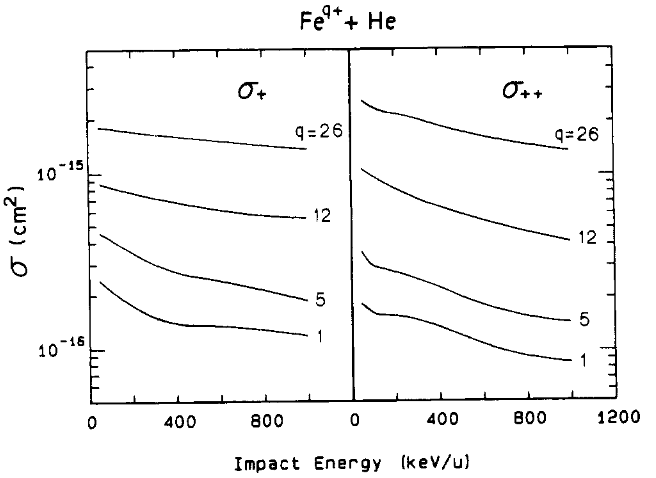

Fig. 3. The total cross section for electron loss (production of He^+ and He^{++}) in collisions of Fe^{q+} and helium for several projectile charge states as a function of impact energy.

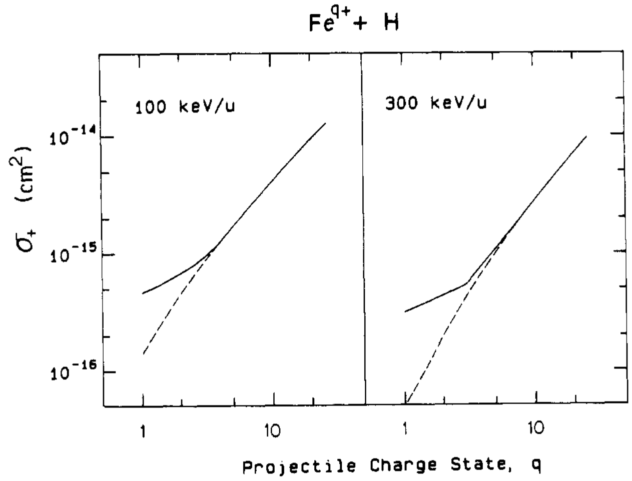

Fig. 5. Dependence of the cross section for electron loss in collisions of Fe^{q+} and atomic hydrogen on projectile charge state at 100 and 300 keV/u impact energy (solid curve) and the dependence for fully stripped ions of charge q (dashed curve).

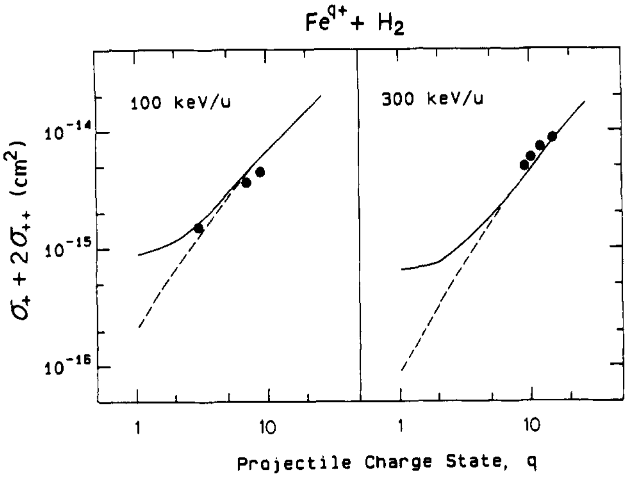

Fig. 6. Dependence of the total electron loss cross section (production of H_2^+ plus H_2^{++}) in collisions of Fe^{q+} and molecular hydrogen on projectile charge state at 100 and 300 keV/u (solid curve) and the dependence for fully stripped ions of charge q (dashed curve). Included are experimental measurements by Berkner *et al.* [15] (solid circles).

penetration is evident in the figure as a levelling off of the electron loss cross section at the lowest charge states, where the electron removed from the target sees practically the same amount of exposed projectile nuclear charge. Therefore, caution should be exericsed in applying the conventional scaling valid for fully stripped ions to the case of impact by low charge state partially stripped ions.

3.2 *He^{2+} + H (n = 1, 2): state selective electron capture*

Another concern of plasma modelers is the determination of the depth of penetration of a neutral beam of atomic hydrogen injected so as to heat the plasma beyond the limits of ohmic heating. Moreover, detailed cross sections for alpha particles provide a framework to diagnose the spatial and energy distributions of the desired product of deuterium–tritium ignition. Such diagnosis is possible by observing the spatial distribution of photons which arise when plasma components capture an electron from the neutral beam atoms to an excited state and subsequently decay. Consequently, a detailed knowledge of the n-level distribution after the capture is necessary so that radiative line intensities may be related to atomic densities. Furthermore, since the neutral beam passes through a dense plasma, it may quite often be excited before suffering ionization or loss by capture. Therefore it is also important to know the distribution of n-levels after capture from excited states of hydrogen. To meet these needs, we present here calculations of such product n-level distributions for collisions of the fusion alpha particles with atomic hydrogen.

To provide a ready point of comparison with experiment and other theoretical treatments we display in Table I the total cross section for capture to He^{2+} from both the ground and $n = 2$ states, summed over all final states as a function of

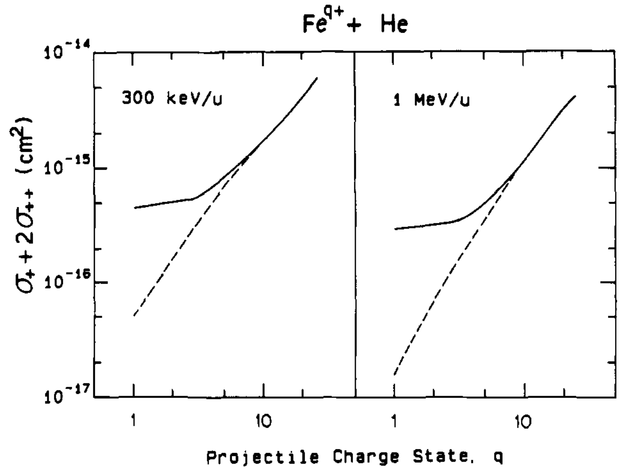

Fig. 7. Dependence of the total electron loss cross section (production of He$^+$ plus He^{++}) in collisions of Fe^{q+} and helium on projectile charge state at 300 and 1000 keV/u (solid curve) and the dependence for fully stripped ions of charge q (dashed curve).

Table I. *The total cross section for capture to all states from the ground and $n = 2$ states of atomic hydrogen by He^{2+} as a function of impact energy, (given in units of 10^{-16} cm^2 with two standard deviation error limits)*

E(keV/u)	$\sigma(1s - \Sigma)\Delta\sigma$	$\sigma(2 - \Sigma)\Delta\sigma$
30	7.43 (0.11)	5.94 (0.24)
40	5.72 (0.10)	2.00 (0.14)
50	4.12 (0.08)	0.86 (0.05)
60	3.86 (0.07)	0.42 (0.03)
80	1.33 (0.04)	0.14 (0.07)
100	0.66 (0.02)	

Table II. *The total cross section for capture to various n-levels from the ground and $n = 2$ states of atomic hydrogen by He^{2+}, (given in units of 10^{-16} cm^2 with two standard deviation error limits)*

30 keV/u			40 keV/u	
n'	$\sigma(1s - n')\Delta\sigma$	$\sigma(2 - n')\Delta\sigma$	$\sigma(1s - n')\Delta\sigma$	$\sigma(2 - n')\Delta\sigma$
1	0.564 (0.028)	0.010 (0.010)	0.520 (0.033)	0.003 (0.006)
2	5.153 (0.148)	0.722 (0.085)	3.305 (0.079)	0.334 (0.048)
3	1.171 (0.052)	1.320 (0.115)	1.189 (0.049)	0.494 (0.070)
4	0.310 (0.020)	1.173 (0.109)	0.417 (0.030)	0.357 (0.060)
5	0.145 (0.042)	0.747 (0.087)	0.186 (0.020)	0.243 (0.049)
6	0.068 (0.009)	0.522 (0.073)	0.098 (0.014)	0.129 (0.036)
7		0.360 (0.030)		0.079 (0.028)
8		0.241 (0.025)		0.068 (0.026)
9		0.195 (0.022)		0.056 (0.022)
10		0.114 (0.017)		0.028 (0.016)
50 keV/u			60 keV/u	
n'	$\sigma(1s - n')\Delta\sigma$	$\sigma(2 - n')\Delta\sigma$	$\sigma(1s - n')\Delta\sigma$	$\sigma(2 - n')\Delta\sigma$
1	0.424 (0.029)	0.005 (0.004)	0.348 (0.024)	0.010 (0.004)
2	2.162 (0.064)	0.163 (0.021)	1.370 (0.046)	0.105 (0.013)
2	0.890 (0.042)	0.229 (0.025)	0.633 (0.032)	0.095 (0.012)
4	0.374 (0.027)	0.141 (0.019)	0.270 (0.021)	0.068 (0.010)
5	0.170 (0.019)	0.092 (0.016)	0.161 (0.016)	0.046 (0.008)
6	0.096 (0.014)	0.033 (0.012)	0.078 (0.011)	0.021 (0.006)
80 keV/u			100 keV/u	
n'	$\sigma(1s - n')\Delta\sigma$	$\sigma(2 - n')\Delta\sigma$	$\sigma(1s - n')\Delta\sigma$	
1	0.201 (0.016)	0.008 (0.002)	0.124 (0.010)	
2	0.575 (0.026)	0.040 (0.004)	0.283 (0.016)	
3	0.297 (0.019)	0.033 (0.004)	0.132 (0.011)	
4	0.131 (0.013)	0.018 (0.003)	0.064 (0.008)	
5	0.078 (0.010)	0.010 (0.002)	0.037 (0.006)	
6	0.043 (0.007)	0.007 (0.002)	0.018 (0.004)	

impact energy. The calculations for the $n = 2$ state represent the statistical mix of $2s$ and $2p$ substates that should be present in the plasma. Also, we note that the capture cross sections for both intial states peak below the lowest energy in the table and monotonically drop over the range tabulated. In Table II these cross sections are partitioned according to the product n-level in the capture process. The cross sections for capture from the ground state peak at $n' = 2$ and for capture from $n = 2$, at $n' = 3$. Further, as expected, total cross sections for capture from the ground state are considerably larger than from $n = 2$ in this energy regime since impact ionization dominates the electron removal for $H(n = 2)$.

To observe the decay of these excited states formed in capture requires, of course, an means of detecting the photons within the reaction vessel. Thus, a method to measure the transitions producing photons in the visible part of the spectrum, such as the use of fiber optics to conduct the light to a remote detector, has a great advantage over detection of the X-rays emitted by the transitions to the ground state for which no such conduit exists. Significantly, the cross sections for capture to $n' = 3$, for example, for which an optical transition to $n' = 2$ produces a visible light photon, is reasonable large. The table indicates that, for this level (i.e., $n' = 3$) the contribution from capture from the $n = 2$ state is comparable to that for capture from the ground state only for the lowest energies tabulated. For example, at 30 keV/u, the $n = 2$ contribution is about ten percent larger than that from the ground state, but at 80 keV/e, the $n = 2$ contribution is only about ten percent as large as that from the ground state.

4. Summary

Cross sections are provided for plasma fusion modelling for electron loss processes involving collisions of the impurity ions $Fe^{q+}(1 < q < 26)$ with H, H_2 and He at collision energies of 50 to 500 keV/u. Projectile core penetration effects lead to behavior which can not be reduced to a simple q scaling of the cross sections for the lower charge states ($q < 10$). Treatment of the interactions between the partially stripped projectile and the target electrons using a Hartree–Fock model potential has allowed this behavior to be elucidated. Further, cross sections for state selective electron capture by fusion product alpha particles colliding with the ground and $n = 2$ states of neutral atomic hydrogen have been presented. These calculations indicate that optical detection of line radition from the excited capture products is feasible because of the relatively large cross sections for capture to the $n' = 3$ and 4 levels. The cross sections presented show that capture from the $n = 2$ state of hydrogen to these final states of helium ($n' = 3$, 4) are dominant at the lower energies ($\lesssim 30$ keV/u) but rapidly decrease in relative importance at higher energies.

Acknowledgement

The authors gratefully acknowledge the support of the Office of Fusion Research, United States Department of Energy.

References

1. Abrines, R. and Percival, I. C., Proc. Phys. Soc. London **88**, 861 (1966).
2. Olson, R. E. and Salop, A., Phys. Rev. **A16**, 531 (1977).
3. Olson, R. E., Phys. Rev. **A24**, 1726 (1981).
4. Becker, R. L. and MacKellar, A. D., J. Phys. **B17**, 3923 (1984).
5. Olson, R. E., Phys. Rev. **A27**, 1871 (1983).
6. Olson, R. E. and Schultz, D. R., Physica Scripta **T28**, 71 (1989).
7. Reinhold, C. O., Schultz, D. R., Olson, R. E., Toburen, L. H. and DuBois, R. D., J. Phys. **B23**, L297 (1990).
8. Meng, L., Reinhold, C. O. and Olson, R. E., Phys. Rev. **A40**, 3637 (1989); Phys. Rev. **A42**, 5286 (1990).
9. Olson, R. E., Berkner, K. H., Graham, W. G., Pyle, R. V., Schlachter, A. S. and Stearns, J. W., Phys. Rev. Lett. **41**, 163 (1978).
10. Schlachter, A. S., Berkner, K. H., Graham, W. G., Pyle, R. V., Schneider, P. J., Stalder, K. R., Stearns, J. W., Tanis, J. A. and Olson, R. E., Phys. Rev. **A23**, 2331 (1981).
11. Schalacter, A. S., Berkner, K. H. Beyer, H. F., Graham, W. G., Groh, W., Mann, R., Müller, A., Olson, R. E., Pyle, R. V., Stearns, J. W. and Tanis, J. A., Physica Scripta **T3**, 153 (1983).
12. Graham, W. G., Berkner, K. H., Pyle, R. V., Schlachter, A. S., Stearns, J. W. and Tanis, J. A., Phys. Rev. **A30**, 722 (1984).
13. Janev, R. K. and Hvelplund, P., Comments At. Mol. Phys. **11**, 75 (1981).
14. Phaneuf, R. A., Janev, R. K. and Hunter, H. T., Nuclear Fusion Special Supplement **7**, 7 (1985).
15. Berkner, K. H., Graham, W. G., Pyle, R. V., Schlachter, A. S. and Stearns, J. W., Phys. Rev. **A23**, 2891 (1981).